PROCEEDINGS OF SCIENCE

R_{AA} and v_n: relativistic transport approach for charm and bottom quarks toward a more solid phenomenological determination of $D_s(T)$

Salvatore Plumari,[a,b,*] **Maria Lucia Sambataro,**[a,b] **Vincenzo Minissale,**[a,c] **Gabriele Parisi**[a,b] **and Vincenzo Greco**[a,b]

[a] *Department of Physics and Astronomy, University of Catania, Via S. Sofia 64, 1-95123 Catania, Italy*

[b] *Laboratori Nazionali del Sud, INFN-LNS, Via S. Sofia 62, I-95123 Catania, Italy*

[c] *NFN Sezione di Catania, Via Santa Sofia,64 - 95123 Catania, Italy*

E-mail: salvatore.plumari@dfa.unict.it

Quasi-Particle Model (QPM) has provided a good description of the main features of lattice QCD (lQCD) and it play a key for studying heavy quark (HQ) dynamics in ultra-relativistic heavy-ion collisions. It can provide a phenomenological estimation of the HQ diffusion coefficient, $D_s(T)$. In this paper, we investigate the bottom quark dynamics within an event-by-event full Boltzmann transport approach coupled with QPM and followed by a hybrid hadronization via coalescence plus fragmentation. Within this approach we provide predictions for R_{AA} and v_2 of B mesons. Finally, we introduce an extension of QPM, where quark and gluon masses depend on their momentum inspired by Dyson-Schwinger studies and converging toward the current quark mass at high momenta. This extended model denoted as QPM_p, successfully provides a simultaneous quantitative description of both the Equation of State (EoS) and quark susceptibilities.

42nd International Conference on High Energy Physics (ICHEP2024)
18-24 July 2024
Prague, Czech Republic

[*] Speaker

PoS(ICHEP2024)625

1. Introduction

Experimental data from RHIC and LHC have provided compelling evidence for the formation of a Quark-Gluon Plasma (QGP). In the context of QGP studies, charm and bottom quarks have emerged as valuable probes for investigating the system's evolution in ultra-relativistic heavy-ion collisions (uRHIC) [1, 2]. These heavy quarks, produced in the early stages of collisions via perturbative QCD (pQCD) processes, possess sufficiently large masses that their thermalization timescales are comparable to the QGP's lifetime, enabling them to probe the QGP throughout its entire evolution. Once they hadronize into heavy hadrons such as D and B mesons, as well as baryons like Λ_c and Λ_b, these observables retain information about the medium formed. Two key observables in this context are the nuclear modification factor ($R_{AA}(p_T)$) and the elliptic flow coefficient ($v_2(p_T)$). These measurements suggest that charm quarks not only undergo significant interactions within the QGP but also exhibit collective flow behavior, indicating their participation in the dynamics [3–13]. Additionally, recent experimental results at LHC energies have shown an enhancement in heavy baryon-to-meson ratios, such as Λ_c/D^0, first observed in $Pb-Pb$ collisions at top LHC energies and later in high-multiplicity proton-proton (pp) collisions. Several models, including coalescence and fragmentation mechanisms, have been proposed to explain these phenomena [14–21]. In this paper, we present results obtained using an event-by-event transport model that combines a hybrid hadronization approach via coalescence and fragmentation. This model has been applied to study HQ observables in $Pb-Pb$ collisions, successfully describing the R_{AA} and $v_{2,3}$ for D mesons [8, 10–13, 22, 23]. In our approach, non-perturbative interactions are incorporated by coupling the transport model to a Quasi-Particle Model (QPM), which provides a quantitative description of the lattice QCD Equation of State (lQCD EoS) even near the phase transition [24, 25].Recently, this model has been extended to the bottom quark sector, offering predictions for centralities where experimental data are not yet available [9]. To further improve the description of the lQCD EoS and quark number susceptibilities, which tend to be underestimated in the standard QPM, we have introduced a model extension called QPM_p. In this extension, quasi-particle masses explicitly depend on momentum, recovering the correct pQCD limit for current quark masses at high momenta [26]. This extension also incorporates the latest lattice results for the QCD EoS with 2+1+1 dynamical flavors, including charm quarks. Within this framework, we have calculated the HQ spatial diffusion coefficient $D_s(T)$, ensuring consistency with lQCD data. This refined approach provides a more accurate description of both QGP dynamics and the non-perturbative interactions that govern HQ behavior.

2. Transport equation and extended Quasi-Particle model

The evolution of both the QGP bulk and heavy quarks is described by the relativistic Boltzmann equations:

$$\{p^\mu_k \partial_\mu + m^*(x)\partial_\mu m^*(x)\partial^\mu_p\} f_k(x, p_k) = C[f_q, f_g](x, p_k) \quad (1)$$

$$p^\mu \partial_\mu f_Q(x, p) = C[f_q, f_g, f_Q](x, p) \quad (2)$$

Where $C[f_q, f_g, f_Q](x, p)$ represents the relativistic Boltzmann collision integral, while $f_k(x, p)$ is the phase space one-body distribution function for the k-th parton. In our approach the collision integral is also gauged to match viscous hydrodynamics, at fixed $\eta/s \approx 0.1$. For further details about the initial conditions of partons in coordinate and momentum space, see Refs. [8, 9]. To account for the non-perturbative effects in bulk-HQs scattering, we evaluate the collision integral using the QPM approach with a temperature dependent coupling constant $g(T)$ fixed by the lQCD energy density, for details Ref. [24]. Recently, new lattice results for the QCD equation of state with 2+1+1 dynamical flavors are available in literature [27] and we show results for the extended QPM from $2 + 1$ to $2 + 1 + 1$ flavors, including the charm quark. Furthermore, we show results of an extension of the standard QPM, where quasi-particle masses depend not only on temperature $m_{g,q}(T)$ but also on momentum following a similar framework developed by the PHSD group based on Dyson-Schwinger and T-matrix studies Ref. [28, 29]. This modification aims to allow masses to decrease toward current quark masses at high momenta, recovering the pQCD behaviour. This extended model, referred to as QPM_p, can reproduce the lQCD equation of state and lQCD quark susceptibilities data. The functional forms for the quasi-particle masses can be found in Ref. [26, 28, 29].

3. Model results

The only available experimental observables to infer information about B meson production are the nuclear modification factor (R_{AA}) and elliptic flow (v_2) of leptons from semi-leptonic B meson decays in $Pb - Pb$ collisions at $\sqrt{s_{NN}} = 5.02$ TeV. Within the standard QPM, we show a comparison of our model for electrons from B meson decays R_{AA} at 0-10 % centrality class (left plot of Fig. 1) and $v_{2,3}$ at 30-50 % centrality class and provide predictions for B meson R_{AA} at LHC energies (right plot of Fig. 1). The behavior of R_{AA} for B mesons is similar to that observed in the charm sector. The hadronization via coalescence and fragmentation generate a peak shift toward higher momenta. We also show the $v_2(p_T)$ using the two-particle correlation method for both B mesons and electrons from B meson decays. Our results predict a non-zero v_2 for bottom quarks, suggesting that bottom quarks participate in the collective flow similarly to charm quarks. However, the $v_2(p_T)$ of B meson show a lower efficiency of ϵ_2 conversion into v_2 which is about 15% lower in central collisions and 40% lower in the $30 - 50$% centrality class.

The quark number susceptibilities $\chi_q = \frac{T}{V}\frac{\partial^2 lnZ}{\partial\mu_q^2}$, provide insights into the nature of the degrees of freedom near the critical temperature T_c. In the left panel of Fig. 2, it is shown the light χ_u/T^2 and strange χ_s/T^2 quark susceptibilities. The standard QPM, which lacks momentum-dependent quasi-particle masses, significantly underestimates the lQCD data. In contrast, the extended model QPM_p, shows much better agreement with the lattice QCD data for both strange and light quark susceptibilities. This improvement is due to the reduced 'thermal average mass' in QPM_p, providing an additional contribution to the susceptibilities especially near the phase transition. For more details see Ref. [26] where also charm susceptibility is discussed for different temperature parametrization of charm quark mass.

In right panel of Fig. 2, we compare the temperature dependence of the spatial diffusion coefficient $D_s(T)$ in both QPM and the extended QPM_p models with lattice QCD (lQCD) data. We found that the QPM_p, which accurately describes both the equation of state (EoS) and quark number susceptibilities, shows a significantly better agreement with the recent lQCD data from Ref. [32], which includes dynamical fermions, as opposed to the standard QPM. For $T \lesssim T_c$, the spatial

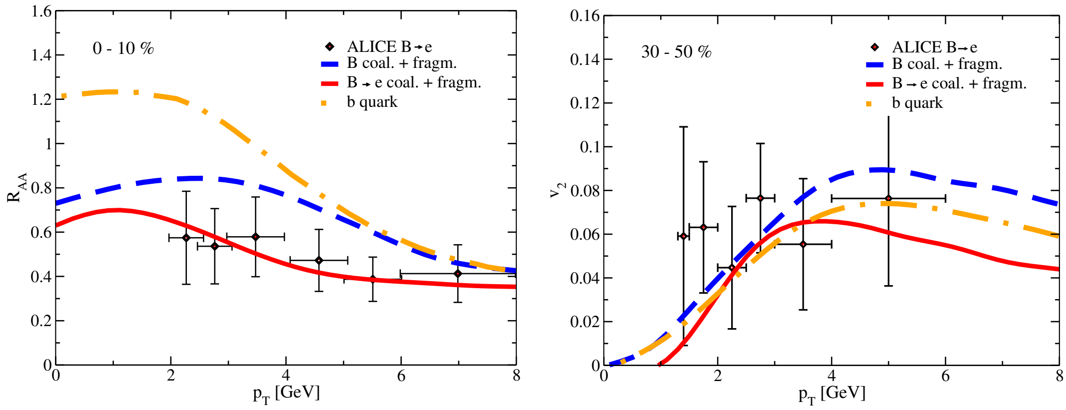

Figure 1: $R_{AA}(p_T)$ (left panel) and elliptic flow $v_2(p_T)$(right panel) for B mesons (blue dashed lines), electrons from B mesons decay (red solid lines) and bottom quarks (orange dot dashed lines) in $Pb-Pb$ collisions at $\sqrt{s} = 5.02$ TeV for two different centrality class. The data are taken from Ref. [30, 31]

diffusion coefficient D_s calculated within the extended model QPM_p shows a pronounced decrease in the low-temperature region ($T < T_c$), while it rises toward the pQCD estimate more rapidly than the standard QPM at higher temperatures. This behavior can be attributed to the effective coupling in the QPM_p model which is stronger than that of the standard QPM at low temperatures.

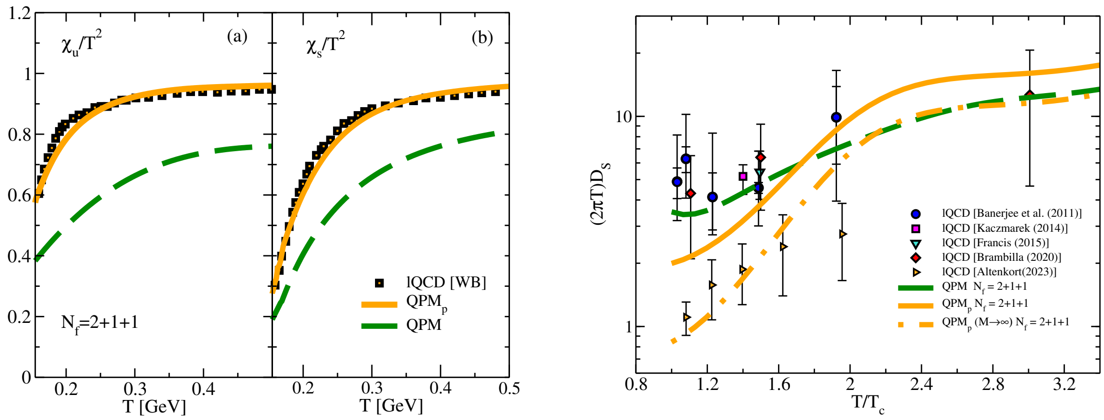

Figure 2: (Left panel) Light (a) and strange quark (b) susceptibility $\chi_{u/s} = \frac{T}{V}\frac{\partial^2 lnZ}{\partial\mu^2_{u/s}}$ for both QPM (green dashed lines) and QPM_p (orange solid lines) with $N_f = 2+1+1$ flavors compared to lQCD data from Ref. [27]. (Right panel) The spatial diffusion coefficient $2\pi T D_s(T)$ plotted as a function of T/T_c in both QPM and QPM_p. Same legend as in the left panel. The Orange dot dashed line refer to the case of QPM_p in the limit of infinite mass. The data points represent lQCD results taken from ref. [32–36].

4. Conclusion

We have studied the bottom quark dynamics in the Quark-Gluon Plasma at top LHC energies using an event-by-event Boltzmann transport approach, coupled with Quasi-Particle Model and with hybrid hadronization via coalescence and fragmentation. Our results for the nuclear modification factor $R_{AA}(p_T)$ and elliptic flow $v_2(p_T)$ of electrons from B meson decays are in agreement with

ALICE experimental data. Furthermore, we have explored an extended Quasi Particle model called QPM_p, where partonic masses depend on momentum, enabling the model to reach the pQCD limit at high momentum. This extension provides a more accurate description of lattice QCD results for the equation of state (EoS), quark number susceptibilities, and the heavy quark diffusion coefficient $D_s(T)$. Future studies will focus on assessing whether QPM_p improves the description of heavy-flavor observables in realistic simulations.

References

[1] X. Dong and V. Greco, *Prog. Part. Nucl. Phys.* **104** (2019) 97.

[2] M. He, H. van Hees and R. Rapp, *Prog. Part. Nucl. Phys.* **120** (2023), 104020.

[3] P.B. Gossiaux and J. Aichelin, *Phys. Rev. C* **78** (2008) 014904

[4] M. He, R.J. Fries and R. Rapp, *Phys. Rev. Lett.* **110** (2013) 112301

[5] J. Uphoff, O. Fochler, Z. Xu and C. Greiner, *Phys. Lett.* **B717** (2012) 430

[6] S. Cao, G.-Y. Qin and S.A. Bass, *Phys. Rev.* **C92** (2015) 024907

[7] A. Beraudo, A. De Pace, M. Monteno, M. Nardi and F. Prino, *JHEP* **05** (2021) 279

[8] M.L. Sambataro, Y. Sun, V. Minissale, S. Plumari and V. Greco, *Eur. Phys. J. C* **82** (2022) 833

[9] M.L. Sambataro, V. Minissale, S. Plumari and V. Greco, *Phys. Lett. B* **849** (2024) 138480

[10] F. Scardina, S.K. Das, V. Minissale, S. Plumari and V. Greco, *Phys. Rev.* **C96** (2017) 044905

[11] S. Plumari, G. Coci, V. Minissale, S.K. Das, Y. Sun and V. Greco, *Phys. Lett. B* **805** (2020) 135460

[12] Y. Sun, S. Plumari and V. Greco, *Eur. Phys. J. C* **80** (2020) 16

[13] L. Oliva, S. Plumari and V. Greco, *JHEP* **05** (2021) 034

[14] Y. Oh, C.M. Ko, S.H. Lee and S. Yasui, *Phys. Rev. C* **79** (2009) 044905

[15] S. Plumari, V. Minissale, S.K. Das, G. Coci and V. Greco, *Eur. Phys. J.* **C78** (2018) 348

[16] S. Cho, K.-J. Sun, C.M. Ko, S.H. Lee and Y. Oh, *Phys. Rev. C* **101** (2020) 024909

[17] M. He and R. Rapp, *Phys. Rev. Lett.* **124** (2020) 042301

[18] V. Minissale, S. Plumari and V. Greco, *Phys. Lett. B* **821** (2021) 136622

[19] A. Beraudo, A. De Pace, D. Pablos, F. Prino, M. Monteno and M. Nardi, *Phys. Rev. D* **109** (2024) L011501

[20] V. Minissale, S. Plumari, Y. Sun and V. Greco, *Eur. Phys. J. C* **84** (2024) 228

[21] J. Zhao, J. Aichelin, P.B. Gossiaux and K. Werner, *Phys. Rev. D* **109** (2024) 054011

[22] S. Plumari, *Eur. Phys. J.* **C79** (2019) 2.

[23] Y. Sun, S. Plumari and S.K. Das, *Phys. Lett. B* **843** (2023) 138043

[24] S. Plumari, W.M. Alberico, V. Greco and C. Ratti, *Phys.Rev.* **D84** (2011) 094004

[25] M.L. Sambataro, S. Plumari and V. Greco, *Eur. Phys. J. C* **80** (2020) 1140

[26] M.L. Sambataro, V. Greco, G. Parisi and S. Plumari, *Eur. Phys. J. C* **84** (2024) 881

[27] S. Borsanyi et al., *Nature* **539** (2016) 69

[28] H. Berrehrah, W. Cassing, E. Bratkovskaya and T. Steinert, *Phys. Rev. C* **93** (2016) 044914

[29] H. Berrehrah, E. Bratkovskaya, T. Steinert and W. Cassing, *Int. J. Mod. Phys. E* **25** (2016) 1642003

[30] ALICE collaboration, *Phys. Rev. C* **108** (2023) 034906

[31] ALICE collaboration, *Phys. Rev. Lett.* **126** (2021) 162001

[32] HotQCD collaboration, *Phys. Rev. Lett.* **130** (2023) 231902

[33] D. Banerjee, S. Datta, R. Gavai and P. Majumdar, *Phys. Rev. D* **85** (2012) 014510

[34] O. Kaczmarek, *Nucl. Phys. A* **931** (2014) 633

[35] A. Francis, O. Kaczmarek, M. Laine, T. Neuhaus and H. Ohno, *Phys. Rev. D* **92** (2015) 116003

[36] N. Brambilla, V. Leino, P. Petreczky and A. Vairo, *Phys. Rev. D* **102** (2020) 074503